Passive Detection and Active Interrogation for Nuclear Disarmament Verification - Outcomes and Challenges from Canadian Technology Demonstration Exercises

G. Li, F. Ali, G. Edwards, H. Fritzsche, O. Kamaev, L. Li, D. Pérez-Loureiro, E. T. Rand, K. Stoev, and B. Sur
Canadian Nuclear Laboratories, Chalk River ON, K0J1J0, Canada

ABSTRACT

Nuclear Disarmament Verification (NDV) requires reliable technologies and procedures to verify nuclear weapons reduction without the transfer of sensitive information. Key challenges include (1) authenticating the presence or absence of well-shielded nuclear weapon material, and (2) preventing "cheating" by the disarming state. As non-nuclear and nuclear weapons states are conscious and supportive of the need to address NDV challenges, several international forums have been initiated to discuss and demonstrate the feasibility of proposed NDV methodologies. Exercises have been conducted worldwide to demonstrate technologies, and to test NDV concepts and procedures. Canadian Nuclear Laboratories (CNL) recently held a technology demonstration exercise for three passive detection technologies – Muon Scattering Tomography, Neutron counting, and Gamma-Ray spectroscopy – to verify nuclear material inside mock-ups of nuclear weapons without determining any sensitive design information. This exercise demonstrated that the complementary information provided by the simultaneous application of the three passive techniques could be used to verify the presence of nuclear material in scenarios where any one of the techniques used in isolation could be defeated. However, there still remain challenges in verifying the presence and absence of nuclear material in plausible shielding and concealment configurations. As a result, CNL is undertaking an active interrogation technology demonstration exercise, to explore the efficacy of neutron and gamma interrogation techniques for verifying the presence and absence of nuclear material in NDV scenarios. In this paper, the results and challenges of the passive technology demonstration exercises will be presented as well as prospective measurement scenarios and simulation results for the active interrogation exercise.

1. INTRODUCTION

Nuclear disarmament verification (NDV), which refers to the use of technology and procedures to verify nuclear weapons elimination without the transfer of sensitive information, is currently a major worldwide initiative. NDV is seen as an important step that the international community can take to make progress on disarmament. A simple nuclear disarmament scenario starts with removal of a warhead from a delivery vehicle (e.g., missile), followed by the removal and separation of high explosives and fissile material from the weapon (which is composed of either highly enriched weapons-grade uranium (WGU) or weapons-grade plutonium (WGPu). The final step is the eventual storage of the fissile material in an internationally monitored facility or transfer to civilian applications. The main dilemma in NDV is the inspectors' requirement to confidently verify the removal of the fissile core while the disarming state - the "Host" - withholds important technological details of the nuclear weapon (via an "information barrier") from the inspectors. The central requirement of an NDV technology is therefore the ability to determine, without revealing sensitive design information, the presence or absence of fissile material.

Although the detailed design of nuclear weapons is secret, the general characteristics of fission weapons are well known. The Fetter model [1] is considered to be the standard reference in many studies in which the properties and behaviour of nuclear weapons are simulated. In this model, an implosion-type fission explosive is represented by a series of concentric spherical shells, with a few kilograms of fissile material on the inside surrounded by a neutron reflector or tamper, a layer of high explosive, and an external case.

The requirement of an “information barrier” during NDV inspections and the multi-layered and relatively complex structure of weapons leads to the consideration of intentional diversion of nuclear materials or “cheating” by the host state and the efficacy of the proposed NDV technology to distinguish genuine nuclear weapons and components from “hoaxes”. Hoaxes may be perpetrated in a number of ways, e.g., by replacing some or all of the weapons grade nuclear material with reactor grade nuclear material, with natural or depleted Uranium, or with heavy metal; by replacing nuclear material with non-nuclear material in conjunction with gamma or neutron sources; adjusting the neutron and gamma shielding provided by the various layers; or by manipulating the geometrical arrangement of materials in ways that would mislead the NDV technology being used.

To probe the efficacy of passive detection technology for the purpose of NDV, CNL undertook a technology demonstration exercise in which three techniques were evaluated: Gamma-Ray spectroscopy (GRS), Neutron counting (NC) and Muon Scattering Tomography (MST).

2. PASSIVE DETECTION TECHNOLOGY DEMONSTRATION

The technology demonstration was completed using a simplified mock-up of a nuclear weapon. It consisted of a hollow steel cube that was designed such that its thickness could be varied from 1.27 cm to 12.7 cm in increments of either 1.27 cm or 2.54 cm. The steel cube acted as a surrogate of the outer shells of the Fetter model, that is, the reflector, the explosive, and the metal casing (see Figure 1). For the muon tomography experiments, the nuclear material core was represented by a plain tungsten cube with a side length of 9 cm and mass of ~14 kg. For the gamma-ray/neutron measurements, a sample of reactor-grade plutonium (RGPu) oxide powder was used. The mass of the plutonium oxide sample was limited to 200 g for safety reasons; such a quantity is equivalent in terms of spontaneous fission neutron and gamma-ray emission rates to several kilograms of WGU [1].

2.1 Neutron / Gamma-Ray Detection Experiments

Gamma-ray and neutron detection limits for various shielding configurations were measured using a liquid scintillator (LS) detector. The energy-calibrated LS detector consisted of a cylindrical LS cell with a diameter of 12.7 cm and length of 15.2 cm, coupled to a photomultiplier tube. The LS material was the commercial product EJ-309 provided by Eljen Technology [2]. Gamma-ray vs. neutron event identification was achieved via the pulse shape discrimination (PSD) parameter, which is the ratio of the tail component to the total signal [3].

Gamma-ray and neutron count rates are shown in left and right panels of Figure 2, respectively. For a typical two-minute acquisition time, the statistical uncertainty in the counts is on the order of 0.3% for gamma events and 5% for neutron events. The RGPu sample is highly radioactive (~2 rem/h near-contact), so even with 1.27 cm of steel shielding the LS detector was saturated. Therefore, neutron and gamma results for an unshielded and a 1.27 cm thick steel cube are not reported here. As expected, the gamma-ray count rate decreases exponentially with the steel thickness; the difference is almost a factor of 20 when the steel shielding thickness is increased from 2.54 to 12.7 cm. For the thickest steel shielding, the gamma count rate is only 11% higher than the background. Because steel is not a good shielding material for neutrons, the neutron count rate decreases much more slowly than the gamma count rate. An increment in the steel thickness from 2.54 to 12.7 cm decreases the neutron count rate by a factor of only 4. Even with 12.7 cm of shielding, the neutron count rate is still 20 times higher than background. However, the addition of 10.2 cm of a hydrogen-rich material such as high-density polyethylene (HDPE) surrounding the steel shielding, which mimics the explosive surrounding the fissile core, reduces the neutron count rate to be similar to that of the background. The effectiveness of gamma and neutron shielding using steel and HDPE is clear. Better shielding effects can be achieved with higher-atomic-number materials (e.g., tungsten) for gamma rays, and by adding thermal neutron absorbers, namely boron or cadmium, to the HDPE moderator. With an optimized shielding configuration, both neutron and gamma signals can easily be masked, and the decision on the presence or absence of fissile material behind the information barrier is difficult to make.

Figure 1: Mock-up used for neutron/gamma-ray measurements (left) and muon scattering experiments (right). Front and top layers removed to show inner samples.

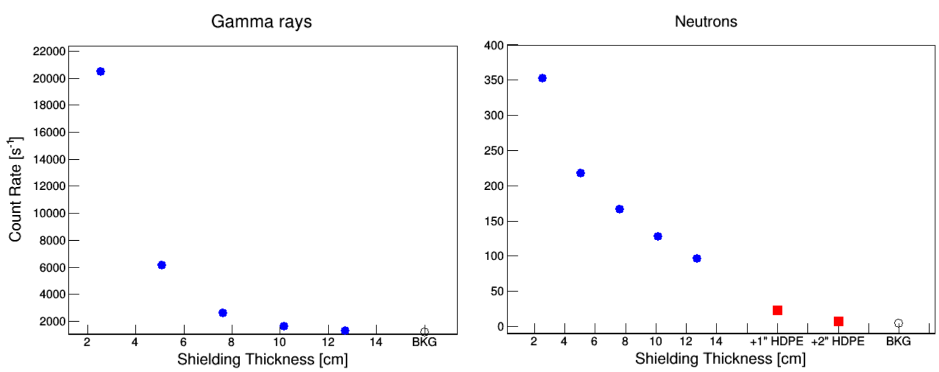

Figure 2: Gamma-ray (left) and neutron (right) count rates measured for the RGPu sample for different steel shielding thicknesses (blue circles). For neutrons, the additional points are for HDPE (red squares). BKG indicates the background count rate (open circles)

2.2 Muon Scattering Tomography Experiments

To systematically investigate the sensitivity of the MST technique to the detection of shielded high-density and high-Z materials, the hollow steel cube mock-up was placed in the centre of the scanning volume of the Cosmic-Ray Inspection and Passive Tomography (CRIPT) system [4]. As in the neutron/gamma-ray experiments, each shielding configuration was scanned with the tungsten cube inside (test case) and without the tungsten cube (reference case). Muon events were selected from the triple coincidence between the two muon trackers and the spectrometer. The spectrometer was used only to provide a cut in the angular acceptance of the incoming muons. Assuming a single muon scattering event occurs in the volume, the Point of Closest Approach (PoCA) algorithm returns the location of the scattering point, the 3D scattering angle, and the distance of closest approach based on the incoming and outgoing muon trajectories. From this information the scattering density estimate (SDE) at each scattering point is calculated and used to map the object under investigation.

Examples of MST images for the 10.2 cm thick shielding scenarios after 48 h of scanning are shown in Figure 3. The MST images were obtained using 1×1×1 cm3 voxels, and therefore no meaningful details of the object could be revealed. This is the minimum voxel size that can be used owing to the angular resolution of the CRIPT system [4]. The right panel, corresponding to the test case, presents a high-density spot in the centre of the image, indicating the presence of the tungsten cube. Results are similar for all the other shielding thicknesses when the entire 48 h acquisition time is used. However, below a threshold scanning time that depends on the shielding thickness, it is not possible to distinguish between the test and reference cases.

If MST images are deemed to reveal unwanted details of the fissile core, a newly developed quantitative method based on non-parametric statistical tests could be used instead. This non-parametric dense object detection algorithm was developed [5] specifically for such situations, and could be made autonomous for computer recognition of heavy elements in various geometries. The non-parametric dense object detection algorithm applies an Anderson–Darling statistical test [6]. It compares histograms of the SDE between the Test and Reference cases to return the probability (p-value) of two samples being drawn from the same original distribution.

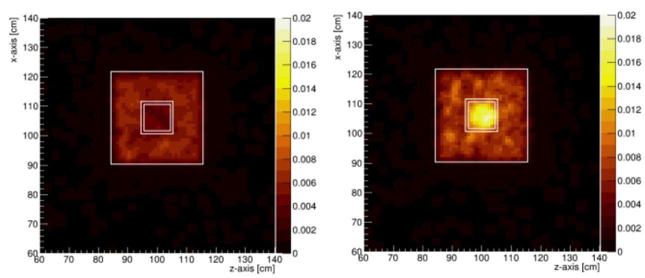

Figure 3: Vertical projection of the reconstructed MST images for the 10.2 cm thickness for reference case (left) and test case (right). The scanning time is 48 h and the voxel size is 1×1×1 cm3. The colour scale corresponds to the SDE in arbitrary units.

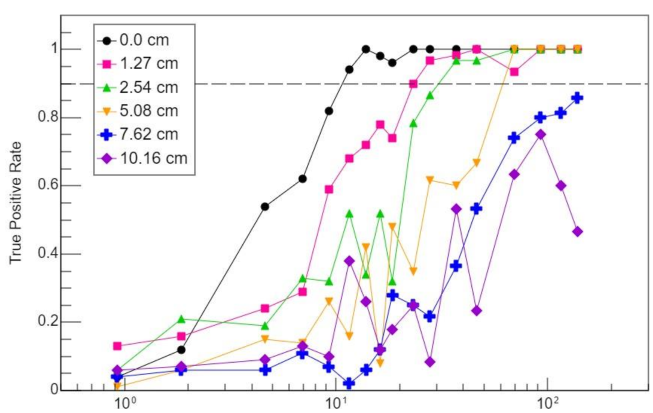

Figure 4: True positive rates obtained with CRIPT detector (experimental measurements) for the detection of a W core in the configurations with various steel shielding from 0 (no shielding) to 10.16 cm as a function of data acquisition time. False positive rate was fixed at 0.1.

Figure 4 summarizes experimental measurements using muon scattering tomography to detect a high-density high-Z tungsten cube inside steel shielding of various thicknesses. For a fixed False Positive Rate (FPR) of 0.1, the True Positive Rate (TPR) of the detection increases with data acquisition time, and the maximum possible value of 1 is reached within relatively short scan times (< 70 min) for the cases of shielding thickness 5.1 cm or less. Cases with increasing steel shielding show a trend of TPR increasing with time and achieving a 90% success rate within the experimental measurement time. Based on a simple extrapolation (not shown here), about 13 hours would be needed to achieve a 90% success rate for 12.7 cm steel shielding.

2.3 Conclusions from Passive Detection Technology Demonstration

The technology demonstration investigated the strengths and limitations of three possible passive detection techniques for NDV. Results with gamma-ray and neutron detectors showed that the number of gamma rays and neutrons emitted by the nuclear material present in the core can be heavily attenuated by the other components of the nuclear warhead. Whereas gamma-ray attenuation is mainly due to a high-density tamper, neutrons can be significantly reduced by the presence of the hydrogen-rich materials. Moreover, additional shielding of the container would make the detection of an armed nuclear warhead more challenging. The MST technique is capable of detecting the presence of a high-density core even when it is heavily shielded. However, no information on the nature of the core material can be provided, and a nuclear weapon in which the nuclear material core is swapped with a tungsten surrogate (to mislead or spoof an inspection) will produce a similar signal. The combination of MST measurements with gamma and neutron detection appears to be the optimal approach. For mock-up warheads (such as the one employed in this study) in which the fissile core is replaced by a high density material such as tungsten, the MST measurements will be able to determine the presence of only a high-density material in the container. However, the absence of gamma-ray and neutron signatures will cast doubt on the nuclear nature of the core. Another challenging scenario would include only surrogate radioactive sources to mimic the radiation signature of the nuclear core. In this case, gamma or neutron detectors would detect the presence of the radioactive materials, but MST would show no high-density material. Positive identification of heavily shielded nuclear materials and identification of spoofs made with a combination of non-nuclear heavy metals combined with gamma and neutron sources remain challenging for the passive detection techniques explored in this demonstration.

3. ACTIVE INTERROGATION TECHNOLOGY DEMONSTRATION

CNL has undertaken a new technology demonstration exercise under the umbrella of a Canadian Safety and Security Program project titled “Exploring applicability of active interrogation techniques for nuclear disarmament verification”. This project objectives are to follow up on the recommendations of the previous Passive Detection technology demonstration by (1) creation of several mock-ups representing the most challenging diversion scenarios in NDV and (2) investigating the application of at least two active interrogation techniques for NDV.

Towards the first objective, the project has assembled a suite of radioactive, nuclear, non-nuclear and shielding materials that can be flexibly configured to provide a variety of scenarios for NDV testing, as detailed in Section 3.1. Radiation sources including Deuterium- Deuterium (DD) and Deuterium-Tritium (DT) neutron generators, x-ray generators and an e-linac are available for active interrogation demonstrations on-site or near site at CNL. Gamma and neutron detection systems configured for special nuclear material detection and identification, in conjunction with the irradiation sources, are also available for the demonstration. Simulation results indicative of the performance of some combinations of sources and detector systems with different active interrogation techniques are also provided in the following sections.

3.1 Mock-ups for NDV Using Active Interrogation Techniques

Five sample components (including four nuclear materials and one non-nuclear material) and four shielding conditions were selected for building the mock-ups so that a number of the “hoax” scenarios enumerated in Section 1 are covered. A short description of the samples and the shielding conditions are presented in Table 1 and Table 2.

Table 1: Selected uranium, plutonium, and tungsten samples for building the mock-ups.

Samples	Material	Shape	Quantity	Total Mass (g)
S1	Depleted uranium (DU)	Solid metallic cube: 3 cm side	Up to 27	15,000
S2	Highly enriched uranium (HEU)	Metallic foil	1	35.10
S3	Highly enriched uranium (HEU)	Metallic hollow tube	1	81.33
S4	Reactor-grade plutonium dioxide (RGPu)	Powder in a plastic bottle	1	50
S5	Tungsten (W)	Solid metallic cube: 3 cm side	Up to 27	15,000

Using the selected samples and shielding conditions, the project will build several mock-ups for active interrogation experiments and verification of the MC simulations. Limited examples of the envisaged mock-ups are listed in Table 3. Note that two samples are involved in some cases. For mock-up M3, there can be n1 number of S1 cubes and n5 number of S5 cubes where the sum of n1 and n5 can be up to 27. For mock-up M10, there can be n1 number of S1 cubes placed in the middle of S3 tube, where the number is limited by the space permitted.

Table 2: Neutron and gamma-ray shielding materials for building the mock-ups.

Shielding	materials	Description
H1	None	The samples are held on a 10 cm × 10 cm × 0.5 cm aluminum plate.
H2	Steel	Slabs form a hollow cube with a fixed internal side of 11 cm and a variable thickness from 1.27 to 12.5 cm in increments of either 1.27 cm or 2.54 cm.
H3	High-density polyethylene (HDPE)	Slabs form a hollow cube with a fixed internal side of 11 cm and a variable thickness of 1.27, 2.54, or 5.04 cm.
H4	Steel outside layers and HDPE inside layers	On the inside, slabs of HDPE form a hollow cube with a fixed internal side of 11 cm and a variable thickness of 1.27, 2.54, or 5.04 cm. On the outside, layered slabs of steel of 2.54 cm thickness are added. The total shielding thickness (HDPE plus steel) can be up to 12.5 cm.

Table 3: Limited examples of the considered mock-ups for MC simulations and active interrogation experiments.

Mock-up	Sample & shielding combination	Variable(s)	Effect
M1	S1&H1	DU mass	Mass
M2	S1&H2	Shielding thickness	Shielding
M3	S1&S5&H1	DU/W quantity ratio	Composition
M4	S1&H3	Shielding type & thickness	Shielding type
M5	S1&H4	Shielding thicknesses	Multiple shielding
M6	S2&H2	Shielding thickness	Uranium isotopic composition
M7	S3&H4	Shielding thicknesses	Uranium mass
M8	S4&H2	Shielding thickness	Fissile material type
M9	S4&H4	Shielding thicknesses	Shielding type
M10	S1&S3&H1	Quantity of DU cubes	fissile isotopic composition

3.2 Simulation of Delayed Neutron (DN) Technique for NDV

DN detection following neutron activation is one of the active interrogation methods for detecting special nuclear materials. Simulations of DN detection, using MCNP6.2 [3], were performed to study the effect of material compositions and various shielding conditions. The simulations used samples listed in Table 1 and the sample composition was based on the suggested composition data for radiation transport modelling [7]. The shielding geometry was a hollow cube with fixed internal sides of 11 cm and variable thickness up to 5 inch (12.7 cm). The shielding was formed by slabs of high density polyethylene (HDPE) or steel, with thickness of 0.5 or 1.0 inch, per the shielding configurations shown in Table 2.

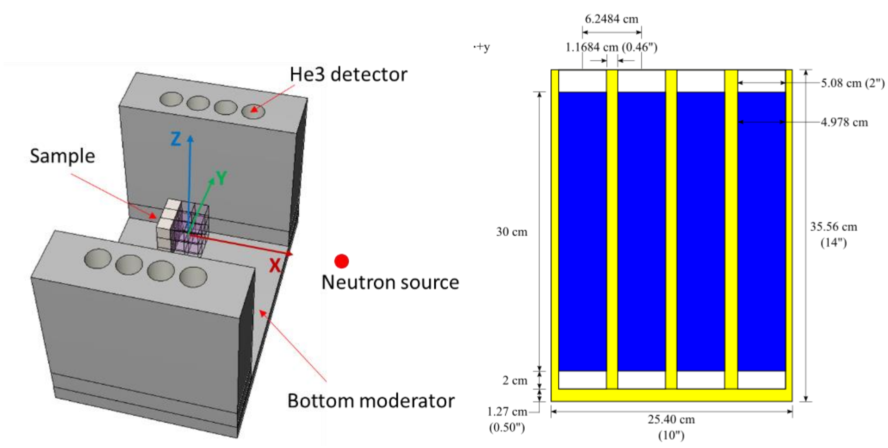

Figure 5: Simulation configuration. (a) Overall setup. This sample shows 18 DU cubes and 9 tungsten cubes. The 5 cm moderator placed below the 3He detectors is shown in the figure, whereas the moderator placed above the 3He detectors is not shown, for the purpose of visualizing the 3He detectors. (b) Detailed dimension of the 3He detectors.

In the simulations, the sample was activated by a DT neutron generator, represented by a point isotropic source with 14.0 MeV energy placed 40 cm away from the center of the sample, and the delayed neutrons were detected by two arrays of ^{3}He detectors, as shown in Figure 5. A 5 cm thick moderator slab made of HDPE was placed above and below the ^{3}He detectors, to moderate fast neutrons. The density of ^{3}He gas in each detector tube was 3.23E−04 g/cm^3. A neutron beam was generated for 1 sec, and the delayed neutrons were recorded starting 0.1 sec after the beam was off to ensure that prompt neutrons would be eliminated. The delayed neutron detection was terminated 120 sec after the beam was off, to represent a practical detection duration.

The effect of shielding with HDPE, steel, and a combination of both was simulated for both DU and HEU samples, and the results are illustrated in Figure 6.

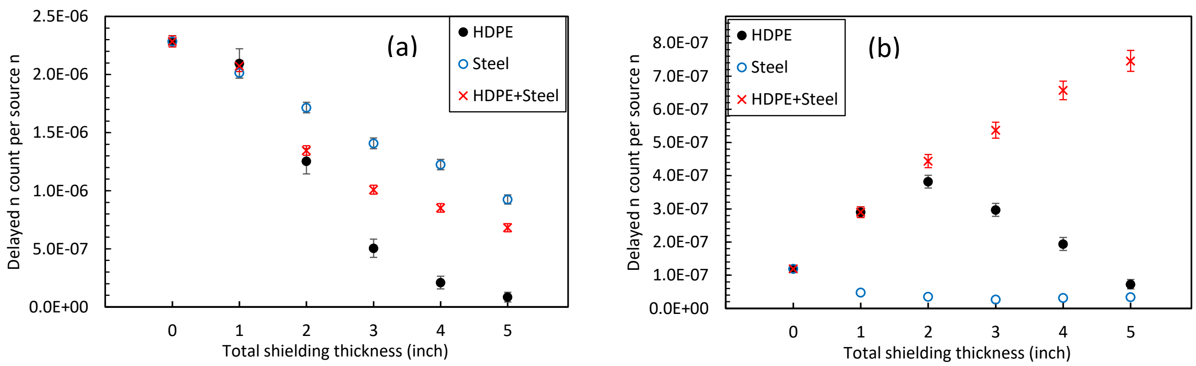

Figure 6: Delayed neutron detection with shielded samples. (a) Sample S1, 27 cubes of DU. (b) Sample S3, HEU.

DU and HEU have large differences in fission cross-section, depending on neutron energy and therefore the shielding effects exhibited different behaviours, especially when HDPE layers were present. For DU, delayed neutron detection was reduced in all three configurations. The HDPE shielding at the maximum 5 inch thickness caused the largest effect, because HDPE also acted as a neutron moderator and DU has a lower fission reaction cross section with low-energy neutrons.

For HEU, the shielding effects were more complicated because of the increased fission reaction cross section with thermalized neutrons. When the shielding was composed of pure steel, the shielding effect showed similar trends for HEU and DU, because steel has little moderation effect. When the shielding was composed of pure HDPE, the delayed neutron detection initially increased with HDPE shielding, up to a 2 inch thickness, and then continuously decreased. The initial increase was caused by the neutron moderation effect from HDPE. Beyond the 2 inch thickness, at which point the thickness was already sufficient to thermalize neutrons, extra thickness would cause more absorption and therefore reduce the delayed neutron detection. When the shielding was a combination of HDPE and steel, the delayed neutron detection continuously increased with more shielding. In this case an increase in thermal neutron flux on sample, primarily due to fast neutron reflection from the outer steel casing competed with attenuation of neutrons by the shielding materials.

3.3 Neutron Resonance Transmission Analysis (NRTA) and Differential Die-Away (DDA) techniques

The NRTA technique, described in Ref. [8], seeks to exploit the resonances in the microscopic fission cross section of fissile isotopes of interest in order to identify the fissile isotope(s) present in the interrogated object.

The DDA technique [9] requires the use of an electronic neutron generator whereby the cavity that contains the interrogated sample is surrounded by thermal neutron detectors embedded in moderating media (for example HDPE). The generator is turned on for several or tens of microseconds and then switched off. The counts recorded in the thermal neutron detectors as a function of time after the generator is switched off is measured. If the resultant counts vs. time plot has two distinct regions with differing exponential decay constants, this is indicative of the presence of fissile material in the interrogated object. If the resultant plot has the shape of a single decaying exponential function, this indicates that there are no fissile materials present in the interrogated object.

The simulations for the proposed CNL configurations indicated that the NRTA and DDA techniques work best when a fissile sample, of relatively large mass, is surrounded by a thin shield. Under this circumstance, the neutron interaction rate with the fissile sample is optimized thereby allowing for resonance absorption in the case of NRTA and fission in the case of DDA to take place in the sample. Conversely, a thicker shield scatters neutrons away from the sample and the neutron interaction rate in a small sample is low resulting in reduced signal for both these techniques.

3.4 Nuclear Resonance Fluorescence (NRF) and Multi-energy X-ray (MEX) Absorption Imaging

NRF and MEX absorption imaging are two gamma ray interrogation techniques under investigation. NRF refers to the resonant excitation of an excited state by absorption of electromagnetic radiation and the subsequent decay of this level by emission of gamma radiation. These NRF peaks are isotope specific and occur at energies in the MeV range which makes them difficult to shield. Therefore, detection of NRF intensities could be used to identify shielded Special Nuclear Material (SNM). In order to be able to measure gamma radiation caused by NRF, a photon source is needed that can provide energies in the range from 1.5 to 3 MeV, where the high-intensity NRF peaks of SNM occur [10, 11]. Usually, for these type of experiments, the bremsstrahlung produced by an electron linear accelerator (e-linac) is used in combination with a 100% efficient High Purity Ge detector (HPGe). Preliminary assessment of signal attenuation and count rates in an experimental setup indicate that detection of SNM in most of the proposed mock-ups in Table 3 or of an object similar to Fetter’s model [1] can be achieved in time scales ranging from seconds to an hour with a 10 MeV 1 mA e-linac source. However detection of HEU surrounded by more than 12.5 cm of steel shielding could not be achieved in a reasonable timescale.

MEX absorption spectroscopy or imaging will also require a bremsstrahlung radiation source produced by energetic electrons from a betatron or linac operating at energies of 6 MeV to 10 MeV. Modeling of beam interactions and material identification via detection at three x-ray energies indicate that SNM in the experimental configurations of Table 1 can be detected but it may be difficult to distinguish between effects caused by material thickness as opposed to material types. MEX can be useful as a fast screening technique with follow-on confirmatory techniques in case an anomaly is detected.

4. CONCLUSIONS

The recently concluded Passive Detection technology demonstration evaluated the effectiveness of three detection techniques – gamma-rays, neutrons and MST. It was found that simultaneous application of the three techniques was effective in verifying the presence or the absence of nuclear material in most cases of interest for NDV. However there remained cases where nuclear material was shielded or used in combination with radiation sources where the passive techniques would be challenged for NDV effectiveness. Therefore an active interrogation technology demonstration has been initiated at CNL.

A configurable set of nuclear, non-nuclear and shielding materials has been established for testing the effectiveness of active interrogation techniques for verifying the presence or absence of nuclear materials for NDV and for testing the ability of these techniques to identify hoaxes. Analytical evaluations and Monte-Carlo simulations of several techniques have been carried out in order to guide and focus experimental efforts. The evaluation of active interrogation techniques for NDV is promising and show that the application of some techniques such as DN may be able to overcome the most challenging NDV cases for passive detection, including the detection of heavily shielded HEU for NDV.

5. ACKNOWLEDGEMENTS

The authors would like to thank Ghaouti Bentoumi for his scientific advice and coordinating various research tasks under this project. This work was carried out under a contract from the Canadian Safety and Security Program and the Federal Nuclear Science and Technology Work Plan at the Canadian Nuclear Laboratories.

6. REFERENCES

[1] S. Fetter et al., "Detecting nuclear warheads," *Sci. Glob. Secur.*, **vol. 1**, no. 3–4, pp. 225–253, (1990), doi: 10.1080/08929889008426333.
[2] "Liquid Scintillators - Eljen Technology." https://eljentechnology.com/products/liquid-scintillators (accessed Jan. 19, 2021)
[3] G. Dietze and H. Klein, "Gamma-calibration of NE 213 scintillation counters," *Nucl. Instruments Methods*, **vol. 193**, no. 3, pp. 549–556, (1982), doi: 10.1016/0029-554X(82)90249-X.
[4] V. Anghel et al., "A plastic scintillator-based muon tomography system with an integrated muon spectrometer," *Nucl. Instruments Methods. A*, **vol. 798**, pp. 12–23, (2015), doi: 10.1016/j.nima.2015.06.054.
[5] E. T. Rand, O. Kamaev, A. Valente, and A. Bhullar, "Nonparametric Dense-Object Detection Algorithm for Applications of Cosmic-Ray Muon Tomography," *Phys. Rev. Appl.*, **vol. 14**, no. 6, p. 64032, (2020), doi: 10.1103/PhysRevApplied.14.064032.
[6] T. W. Anderson and D. A. Darling, "A Test of Goodness of Fit," *J. Am. Stat. Assoc.*, **vol. 49**, no. 268, pp. 765–769, (1954), doi: 10.2307/2281537.
[7] R. G. Williams, C. J. Gesh, and R. T. Pagh, "Compendium of Material Composition Data for Radiation Transport Modeling," United States, Oct. 2006. [Online]. Available: http://inis.iaea.org/search/search.aspx?orig_q=RN:42022343 .
[8] Chichester, D.L. and Sterbentz, J.W., "Neutron Resonance Transmission Analysis (NRTA): Initial Studies of a Method for Assaying Plutonium in Spent Fuel" *INL/CON-10-20684*. (2011) Idaho Falls, Idaho: Idaho National Laboratory.
[9] Martinik, T., Henzl, V., Grape, S., Svärd, S.J., Jansson, P., Swinhoe, M.T., and Tobin, S.J.,."Simulation of differential die-away instrument's response to asymmetrically burned spent nuclear fuel" *NIM* **A 788** pp 79 – 85 (2015)
[10] W. Bertozzi et al., *Phys. Rev.* **C 78**, 041601 (2008).
[11] J. R. Vavrek, B. S. Henderson and A. Danagoulian, *Proceedings of the National Academy of Sciences* **115 (17)**, 4363 (2018).